

# Bipolar orientation of chromosomes in *Saccharomyces cerevisiae* is monitored by Mad1 and Mad2, but not by Mad3

Marina S. Lee and Forrest A. Spencer\*

McKusick–Nathans Institute of Genetic Medicine, School of Medicine, The Johns Hopkins University, Baltimore, MD 21205

Communicated by Carol W. Greider, The Johns Hopkins University School of Medicine, Baltimore, MD, June 10, 2004 (received for review March 20, 2004)

**The spindle checkpoint governs the timing of anaphase separation of sister chromatids. In budding yeast, Mad1, Mad2, and Mad3 proteins are equally required for arrest in the presence of damage induced by antimicrotubule drugs or catastrophic loss of spindle structure. We find that the *MAD* genes are not equally required for robust growth in the presence of more subtle kinetochore and microtubule damage. A *mad1Δ* synthetic lethal screen identified 16 genes whose deletion in cells lacking *MAD1* results in death or slow growth. Eleven of these *mad1Δ* genetic interaction partners encode proteins at the kinetochore–microtubule interface. Analysis of the entire panel revealed similar phenotypes in combination with *mad2Δ*. In contrast, 13 panel mutants exhibited a less severe phenotype in combination with *mad3Δ*. Checkpoint arrest in the absence of bipolar orientation and tension (induced by replication block in a *cdc6* mutant) was lacking in cells without *MAD1* or *MAD2*. Cells without *MAD3* were checkpoint-proficient. We conclude that Mad1 and Mad2 are required to detect bipolar orientation and/or tension at kinetochores, whereas Mad3 is not.**

The spindle checkpoint monitors kinetochore–spindle microtubule interaction and blocks sister chromatid separation until all kinetochores have achieved stable bipolar attachment (1). The process of establishing stable chromosome attachment to the mitotic spindle requires that sister kinetochores capture microtubules emanating from opposite spindle poles. Tension across sister kinetochores with bipolar orientation is the result of pulling forces exerted by attached microtubules. These forces are opposed by cohesion of adjacent chromosomal arms. Anaphase onset is allowed once all kinetochores are under tension. This regulatory mechanism ensures that each daughter cell receives a full complement of chromosomal DNA.

Proteins responsible for checkpoint signaling were first identified in budding yeast screens designed to detect genes required for cell-cycle pause in the presence of spindle damage (2, 3). From these original studies, kinetochore-associated proteins Mad1, Mad2, Mad3, Bub1, and Bub3 were identified, and highly conserved orthologous proteins were found throughout the eukaryotic kingdom (1). Subsequent studies have demonstrated a role for the checkpoint proteins in preventing anaphase initiation by inhibiting Cdc20 activation of the anaphase promoting complex (APC) (1). Anaphase is initiated once APC<sup>Cdc20</sup> polyubiquitinates securin (known in budding yeast as Pds1). Degradation of securin results in the release of its binding partner, the cysteine protease separase (budding yeast Esp1). Separase cleavage of several proteins important for mitotic progression ensues, including the Mcd1/Sccl subunit of cohesin (1, 4). Concomitantly, sister chromatid cohesion is released and chromosome segregation to the poles proceeds.

Spindle checkpoint proteins are responsive to both tension and attachment defects of kinetochores (1). In both budding and fission yeast, spindle checkpoint proteins Mad2, Bub1, and Bub3 localize to unattached kinetochores (5–10). Mad3 is seen at unattached kinetochores in fission yeast (7). Mad3 has not been observed at kinetochores in budding yeast cells treated with nocodazole; however, under these conditions, Mad1 is localized

to the kinetochore (9). Vertebrate checkpoint proteins Mad2, Bub1, Bub3, and BubR1 (a Mad3 homolog with a kinase domain) are also found at kinetochores when kinetochore–microtubule attachment is prevented by microtubule-depolymerizing drugs (11, 12). In unaltered prometaphase or during recovery from antimicrotubule drug treatment, Mad2 localization disappears from kinetochores upon capture by microtubules. Once tension is established across sister kinetochores at the metaphase plate, Bub1, Bub3, and BubR1 kinetochore staining diminishes (11, 12).

In *Saccharomyces cerevisiae*, Mad1, Mad2, and Mad3 are found in inhibitory complexes that prevent Cdc20 activation of the APC (1), thereby preventing anaphase initiation upon degradation of Pds1. However, several phenotypes distinguish the functions of Mad1 and Mad2 from that of Mad3. *mad1Δ* and *mad2Δ* mutants exhibit a higher rate of loss for a nonessential chromosome fragment and are more sensitive to the microtubule-depolymerizing drug, benomyl (13). Mad1 and Mad2 also associate with the nuclear pore during interphase (10). Upon treatment with a microtubule-depolymerizing drug, this localization shifts to kinetochores (10). In the absence of Mad3, Mad1/Mad2 still localize to unattached kinetochores (9) and Mad2–Cdc20 complexes can be immunoprecipitated (9, 14). In addition, two kinetochore proteins (Dam1 and Cbf1) and several factors that affect microtubule dimer formation exhibit a more severe genetic interaction with *MAD1* or *MAD2* than with *MAD3* (15–17). These phenotypic differences have suggested that Mad1 and Mad2 provide functions in the cell that are not shared by Mad3.

We present evidence here that *MAD1* and *MAD2* are required for the checkpoint response to absence of spindle tension, whereas *MAD3* is not. A synthetic lethal screen was performed by using the *MATa* haploid yeast knockout (*ykoΔ*) collection (18) and oligonucleotide tag microarray hybridizations to follow viability of *mad1Δ ykoΔ* double mutants (19). The screen identified a panel of mutants with roles in kinetochore structure and microtubule dynamics that require the spindle checkpoint protein Mad1 for robust viability. This panel of mutants was used as a reagent to characterize *in vivo* requirements for *MAD2* and *MAD3*. Synthetic lethal analysis of the panel mutants with *mad2* and *mad3* deletions confirms the presence of a role for Mad1 and Mad2 that is not shared by Mad3. In detailed phenotypic analysis, we find that all three genes are equally required for arrest after microtubule disruption by nocodazole. In contrast, checkpoint arrest caused by absence of a sister chromatid (in the presence of a bipolar spindle) requires *MAD1* and *MAD2* but not *MAD3*. Therefore, Mad1 and Mad2 participate in a bipolar orientation defect signaling pathway, whereas Mad3 does not.

## Methods

**Strains and Media.** Strain genotypes are given in Table 1, which is published as supporting information on the PNAS web site. Media formulations are standard (20, 21).

Abbreviation: APC, anaphase promoting complex.

\*To whom correspondence should be addressed. E-mail: fspencer@jhmi.edu.

© 2004 by The National Academy of Sciences of the USA

**mad1 Synthetic Lethal Screen.** A MATa haploid pool of  $\approx 4,700$  *ykoΔ::KanMX* mutants was transformed with a *mad1Δ::NatMX* deletion cassette, and  $2 \times 10^5$  *Kan<sup>R</sup> Nat<sup>R</sup>* double mutants were selected in each of three independent transformations (Fig. 4, which is published as supporting information on the PNAS web site). After 2 days' growth, colonies were scraped from selective plates and genomic DNA was isolated. Downtag probe was made by PCR (LA Taq, Takara, Shiga, Japan), using Cy-labeled primers. Tag microarrays (gift of D. Shoemaker and J. Boeke, The Johns Hopkins University) were cohybridized with experimental and control probes (22) that were differentially labeled with Cy3 and Cy5 fluorophores.

Microarray images were analyzed in IMAGENE (BioDiscovery, El Segundo, CA) and data were analyzed in R, an open source environment for statistical analysis ([www.r-project.org](http://www.r-project.org)). Log<sub>2</sub>-transformed data were normalized by quantiles (23), and tag ratios (*ura3/mad1*) were calculated for each hybridization. Each ratio was assigned a percentile rank within each experiment, and percentile ranks for each gene were averaged across the six hybridizations to create the final list.

The top 95 putative *mad1Δ*-interacting genes identified by the array-based ratios (Table 2, which is published as supporting information on the PNAS web site) were independently tested in random spore analysis from individual matings. This rescreeing identified 11 synthetic partners of *mad1*, representing both lethal and reduced fitness interactions. All 11 *mad1Δ*-interacting genes identified by the array-based screen have functions that could affect the stability of the kinetochore–microtubule interface. An additional set of nine genes with similar functions was tested (Table 2). Of this list, five mutants have a genetic interaction with *mad1Δ*.

**Random Spore Analysis.** Random spore analysis was performed essentially as by Tong *et al.* (21) except all manipulations were manual. Double-mutant growth defects were determined after 42 h at 30°C by comparison with single mutants. *mad1Δ*, *mad2Δ*, and *mad3Δ* were indistinguishable from wild type in growth. Therefore, *mad1*, 2, 3Δ *ykoΔ* double mutants were compared directly to *ura3Δ ykoΔ* controls. Additionally, the phenotype of all *mad1Δ* and *mad3Δ* combinations with interacting mutants was confirmed by spores obtained from tetrad dissection (Table 3, which is published as supporting information on the PNAS web site). Strain identity and purity were validated by using PCR.

**Kinetics of Nocodazole Response.** Overnight cultures were arrested in G<sub>1</sub> with  $\alpha$  factor for 2.5 h, washed twice, and released into yeast extract/peptone/dextrose plus 15  $\mu$ g/ml nocodazole (Sigma). Time points were taken every 15 min. Aliquots were processed for flow cytometry as by Hanna *et al.* (24). Bud morphology and microcolony viability were scored as by Pangilinan and Spencer (25).

**Response to Tension Defects.** Experiments following Pds1 levels in the absence of DNA replication (*GAL-CDC6* shut-off) were performed essentially as described (26). Overnight cultures were arrested with  $\alpha$  factor for 3 h in YPRG (1% raffinose/2% galactose). Cells were released into YPRG (no  $\alpha$  factor) for 1 h, and then washed into yeast extract/peptone/dextrose (2% dextrose) to shut off transcription from the *GAL-CDC6* allele. Two and a half hours later, cells were released for the time course and aliquots were taken. Proteins were prepared from frozen cell pellets by vortex mixing with glass beads in 5% SDS, followed by boiling. Lysates were cleared with 10-min centrifugation (16,000  $\times$  g). Sample volumes were adjusted after protein quantitation by using DC protein assay (Bio-Rad). Ten micrograms of total protein was loaded in each lane and run on a 10% (30:0.2) acrylamide gel (Invitrogen). Pds1–18myc was detected by using 1:2,000 mouse anti-myc 9E10 (Covance, Princeton), 1:20,000

horseradish peroxidase-conjugated goat anti-mouse (Pierce), and SuperSignal West Pico (Pierce).

## Results

**A Synthetic Lethal Screen for Mutants Requiring MAD1.** The *mad1* synthetic lethal screen used a microarray hybridization-based approach (19) to identify null mutants that exhibited cell death (synthetic lethal) or slow-growth (synthetic fitness) phenotypes in combination with *mad1Δ*. We identified 16 mutants that required *MAD1* for robust viability (Fig. 1). Eleven of these genes were recently reported elsewhere as *mad1* genetic interaction partners from high-throughput serial genetic analysis screens (17), and five have not been previously reported (*CTF3*, *MCM16*, *IML3*, *CHL4*, and *SLK19*).

The 16 genes we identified are annotated in the literature for roles at the microtubule–kinetochore interface. *KAR3* and *CIN8*, which encode motor proteins whose forces oppose each other on the mitotic spindle, exhibit a synthetic lethal interaction with *mad1Δ* (15, 27). The microtubule stability protein, *Bim1*, and the outer kinetochore proteins, *Ctf19* and *Mcm21*, also require *Mad1* for viability (15, 28, 29). Another class of genetic interactions with *MAD1* exhibited synthetic fitness: double mutants formed smaller colonies than either single mutant. In this class, we identify the following genes: *PAC2*, *CIN1*, *CIN2*, *TUB3*, *GIM4*, *MCM16*, *MCM22*, *IML3*, *CHL4*, *CTF3*, and *SLK19*. Five of these (*PAC2*, *CIN1*, *CIN2*, *TUB3*, and *GIM4*) are involved in  $\alpha/\beta$  tubulin heterodimer formation (30–32). *Mcm16*, *Mcm22*, *Iml3*, *Chl4*, and *Ctf3* are outer kinetochore proteins (33) and are peripheral members of the *Ctf19*–*Mcm21* complex (34). Finally, *SLK19* encodes a kinetochore-associated protein that relocalizes to the spindle midzone at anaphase where it is thought to stabilize anaphase spindles (35).

**Mad1 and Mad2 Proteins Function Together.** *Mad1* and *Mad2* form a tight complex throughout the cell cycle and this interaction is crucial for checkpoint function, because alleles of *Mad2* that cannot interact with *Mad1* are checkpoint-deficient (36, 37). Moreover, *mad1Δ*- and *mad2Δ*-null mutants show similar chromosome loss rates (13). To test whether *MAD2* is required by all *mad1*-interacting genes, random spore analysis was performed by crossing the panel of *mad1Δ*-interacting mutants (*MATa ykoΔ::KanMX*) and a tester strain (*MAT $\alpha$  mad2Δ::NatMX*) containing haploid selection markers (*can1 mfa1::MFA1pr-HIS3*). *mad2Δ* double mutants exhibited growth defects indistinguishable from *mad1Δ* double mutants (Fig. 1).

**MAD3 Is Required Only by a Subset of Mutants Requiring MAD1.** *Mad2* and *Mad3* are both members of the *Cdc20* complex, which prevents anaphase onset (14). To test the requirement of *MAD3* in the panel of genes that equally require *MAD1* and *MAD2*, *mad3Δ::NatMX* was introduced by mating. Double heterozygous diploids were sporulated, double-mutant progeny were selected, and relative growth rates were assessed (Fig. 1). Only three genes (*BIM1*, *KAR3*, and *CIN8*) equally require *Mad1* and *Mad3* for viability (15, 28). Seven genes interacted with *mad3Δ* but with less severe phenotypes than were seen with *mad1Δ* or *mad2Δ* (*CTF19*, *MCM21*, *CIN1*, *CIN2*, *PAC2*, *TUB3*, and *GIM4*). The six remaining genes (*CHL4*, *CTF3*, *IML3*, *MCM16*, *MCM22*, and *SLK19*) exhibited no synthetic phenotype with *MAD3*. The genetic interactions seen by random spore analysis were confirmed by double-mutant spore growth from tetrad dissection (examples shown in Fig. 1). These interaction data provide additional evidence that *MAD1* and *MAD2* have functions in the cell distinct from the spindle checkpoint gene *MAD3*.

**Nocodazole Arrest and Recovery: Indistinguishable Phenotypes.** Previous studies have suggested an equivalent requirement for *MAD1*, *MAD2*, and *MAD3* genes in checkpoint arrest after

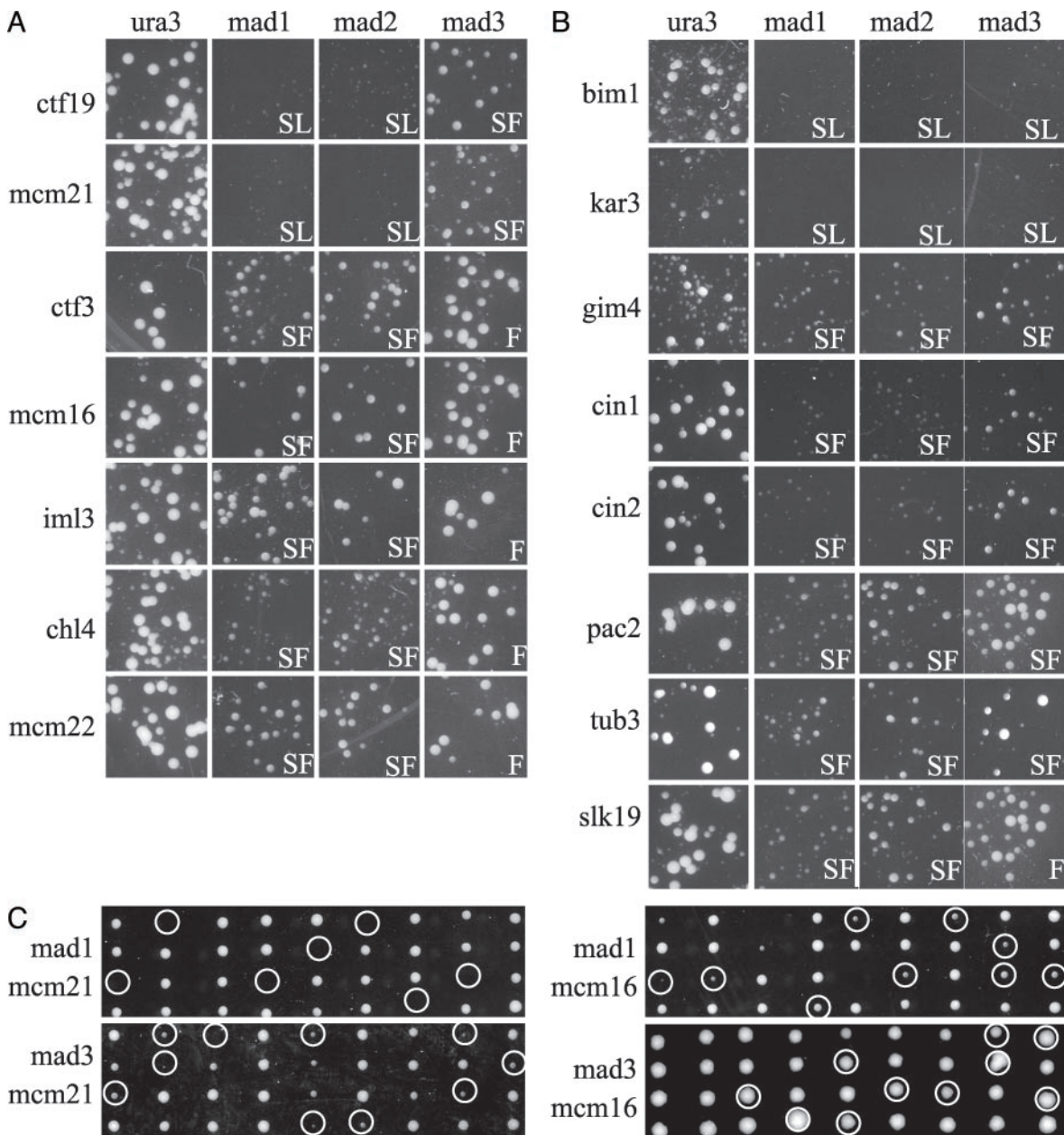


**Fig. 1.** Random spore analysis. *mad1* $\Delta$ , *mad2* $\Delta$ , *mad3* $\Delta$ , and *ura3* $\Delta$  strains exhibit colony growth indistinguishable from the deletion collection parental strain (data not shown). *ura3* $\Delta$  *yko* $\Delta$  double mutants were evaluated to reveal any slow-growth phenotypes of *yko* $\Delta$  mutants (notably *bim1* $\Delta$  and *kar3* $\Delta$ ). (A) Growth of mutants in the outer kinetochore Ctf19 complex in combination with *mad1* $\Delta$  and *yko* $\Delta$  interacting pairs identified is shown. Also shown are the growth phenotypes of these *yko* $\Delta$  mutants in combination with *mad2* $\Delta$  and *mad3* $\Delta$ . *mad* $\Delta$  *yko* $\Delta$  double mutants that do not grow have a synthetic lethal interaction (SL). Synthetic fitness (SF) interactions are seen as reduced colony size in the *mad* $\Delta$  *yko* $\Delta$  double mutant versus *ura3* $\Delta$  *yko* $\Delta$ . Double mutants with no distinguishable growth defect are considered fine (F). (B) The growth phenotypes of the mutants that affect microtubule stability are shown in combination with *ura3* $\Delta$ , *mad1* $\Delta$ , *mad2* $\Delta$ , and *mad3* $\Delta$ . Random spore analysis could not be used to evaluate *cin8* $\Delta$  in double mutant combinations because *cin8* $\Delta$  and *can1* $\Delta$  are closely linked. The previously reported synthetic lethal interactions with *cin8* $\Delta$  (15) were therefore confirmed only by tetrad dissection (Table 3). (C) Examples of tetrad dissections of heterozygous *mad* $\Delta$  *yko* $\Delta$  diploids. Double mutants (inferred or observed) are indicated.

antimicrotubule drug-induced spindle damage (2, 14, 38, 39). However, a few studies have demonstrated a weaker phenotype for *mad3* $\Delta$  mutants (9, 13, 15, 16), indicating there could be residual checkpoint activity in *mad3* $\Delta$  mutants that is provided by the presence of Mad1 and Mad2.

To test whether a weak checkpoint response of *mad3* $\Delta$  cells has been missed in previous experiments, we evaluated the checkpoint response of *mad1* $\Delta$ , *mad2* $\Delta$ , and *mad3* $\Delta$  cells at closely spaced time points after exposure to high concentrations of nocodazole. Checkpoint defects in an isogenic set of null

mutants were evaluated by following three parameters at 15-min intervals in synchronous cultures: new bud formation, recovery after removal of nocodazole, and the timing of DNA re-replication (Fig. 2). Logarithmically growing cultures of *mad1* $\Delta$ , *mad2* $\Delta$ , *mad3* $\Delta$ , and wild type were synchronized in G<sub>1</sub> with  $\alpha$  factor at 30°C, and then released into media containing nocodazole. At each time point, aliquots were spotted onto solid media to assess microcolony viability, fixed and stained with 4',6-diamidino-2-phenylindole for cell morphology, and processed for flow cytometry to follow DNA content.

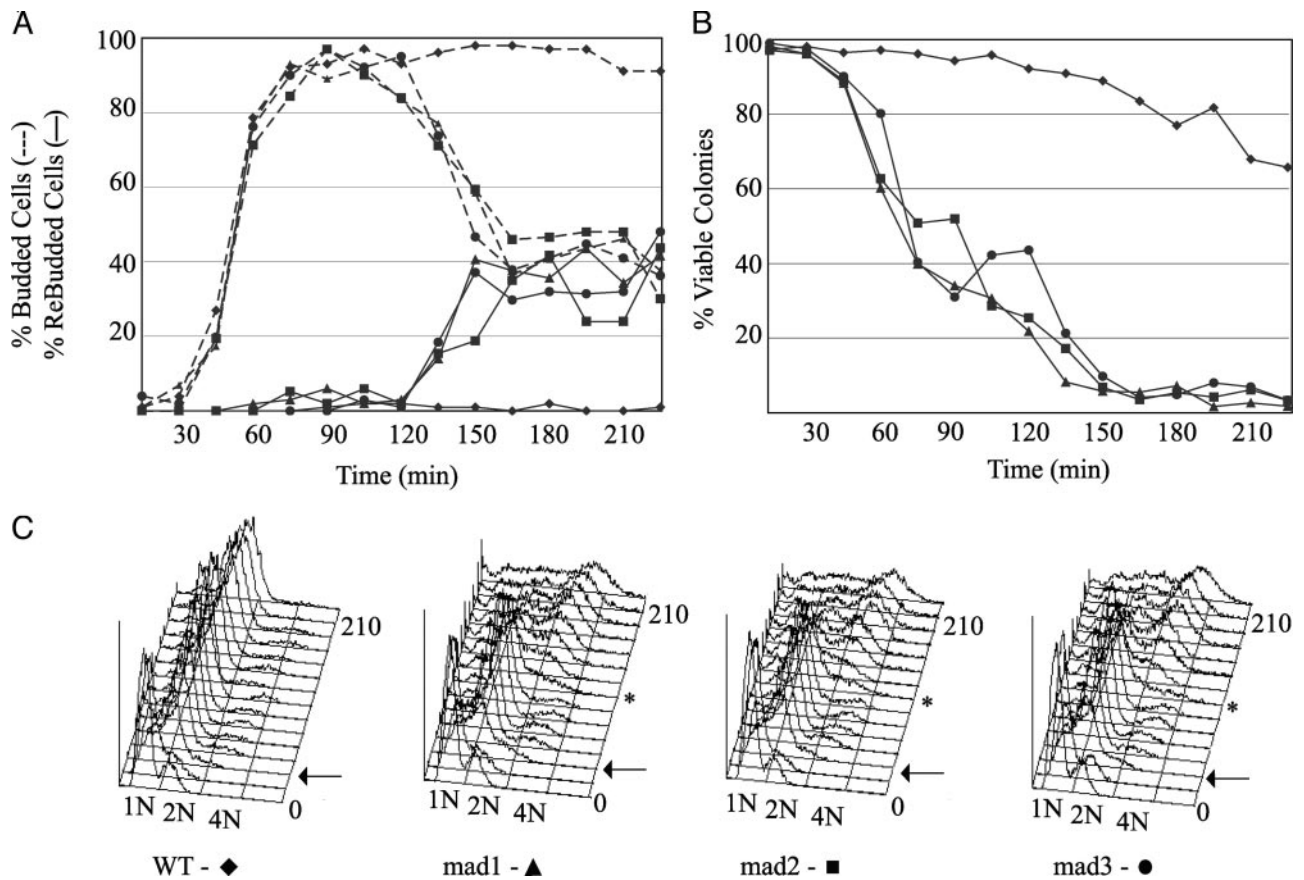


**Fig. 2.** *mad1Δ*, *mad2Δ*, and *mad3Δ* response to nocodazole treatment. Strains were synchronized in G<sub>1</sub> with  $\alpha$  factor and released into nocodazole ( $t = 0$  min). Aliquots were analyzed for cell morphology, viability, and DNA content. (A) Formaldehyde-fixed, 4',6-diamidino-2-phenylindole-stained samples were analyzed for cell cycle by bud morphology. (B) At the indicated times, aliquots were plated on nocodazole-free medium (yeast extract/peptone/dextrose) to evaluate cell viability. The frequency of colony-forming units was determined by microscopic examination 20 h after plating. (C) DNA content was monitored by flow cytometry. Arrows indicate first-cycle DNA replication after  $\alpha$  factor release; \* indicates second-cycle DNA replication in mutants. The experiment was performed twice with similar results.

All cultures exhibited synchronous release from G<sub>1</sub> arrest, as seen by the kinetics of single-bud accumulation (Fig. 2A, dotted lines) and first-cycle DNA replication (Fig. 2C, arrows). *mad1Δ*, *mad2Δ*, and *mad3Δ* mutants could not arrest cells at G<sub>2</sub>/M and proceeded to re-replicate their DNA (Fig. 2C, asterisk), as well as rebud (Fig. 2A, solid lines). All three mutants also showed a rapid decline in ability to recover from nocodazole treatment (Fig. 2B). Cell cycle progression was indistinguishable in all three mutants. This analysis fully confirmed that *mad1Δ*, *mad2Δ*, and *mad3Δ* mutants are equally checkpoint-defective in microtubule-depolymerizing levels of nocodazole.

One interpretation of the genetic interaction partners that equally require *MAD1*, *MAD2*, and *MAD3* is that their null mutations cause spindle damage similar to that induced by nocodazole treatment. Interestingly, the three genes in this group (*BIM1*, *KAR3*, and *CIN8*) are likely to compromise kinetochore capture by virtue of aberrant microtubule plus end dynamic instability. Further, the mutations in genes that exhibit a decreased or no requirement for *MAD3* (*CTF19*, *MCM21*, *CIN1*, *CIN2*, *CHL4*, *CTF3*, *IML3*, *MCM16*, *MCM22*, *SLK19*, and *TUB3*) may cause spindle damage distinct from that induced by nocodazole. Based on this speculation, we tested whether a differential requirement for *MAD1* and *MAD2* versus *MAD3* could be found under conditions where, in the presence of a bipolar spindle, attachment is possible but bipolar orientation and tension is prevented.

**Biorientation/Tension Defects Do Not Require MAD3.** Previous work has established a requirement for *MAD1* and *MAD2* in a cell cycle arrest induced by absence of a sister kinetochore, when DNA replication is prevented by absence of *CDC6* (26, 40). In this configuration, kinetochore capture by spindle microtubules is not prevented, but bipolar attachment and ensuing tension on sister kinetochores cannot be achieved. We tested whether *MAD3* is required for this arrest. *mad1Δ*-, *mad2Δ*-, or *mad3Δ*-null alleles were introduced into a *GAL-CDC6* strain. Log-phase cultures were arrested in G<sub>1</sub> with  $\alpha$  factor in media containing raffinose and galactose, which supported *CDC6* expression (Fig. 3A). Cells were released from G<sub>1</sub> arrest in raffinose-galactose media and at 60 min (which was after S-phase entry for this cycle) were shifted into media containing glucose to repress *CDC6*. These cells were treated, again, with  $\alpha$  factor to arrest cells in G<sub>1</sub> of the next cell cycle, which proceeded in the absence of *CDC6*. Pds1-18MYC levels were monitored by Western blot at time points after the second  $\alpha$  factor release. It was in this cell cycle that DNA replication was blocked, resulting in mono oriented kinetochores without tension, attached to a bipolar spindle.

Cells that were wild type for *MAD1*, *MAD2*, and *MAD3* maintained elevated levels of Pds1p at least 180 min postrelease (Fig. 3B Top). In contrast, *mad1Δ cdc6* and *mad2Δ cdc6* cells rapidly degraded Pds1 (Fig. 3B Middle). These observations confirm previously published results (26, 40). However, *mad3Δ cdc6* cells were able to sustain Pds1 levels for up to 150 min (Fig. 3B Bottom). This maintenance of Pds1 in *mad3Δ cdc6* was

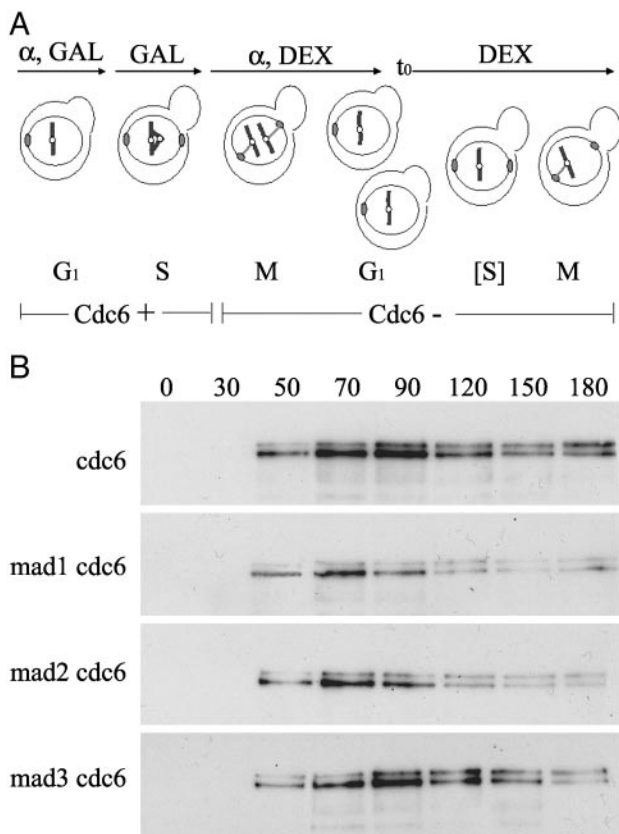


**Fig. 3.** Requirement of *mad1*, *mad2*, and *mad3* for spindle checkpoint delay in response to mono oriented kinetochores. (A) Diagram of method used to generate unreplicated mono oriented kinetochores, as in ref. 26. GAL, galactose; DEX, dextrose. (B) Pds1-18MYC levels were monitored by Western blot. Equal amounts of total protein were loaded in each lane and confirmed by Coomassie staining (Fig. 5, which is published as supporting information on the PNAS web site).

observed in three independent transformants (data not shown). Therefore, *MAD3* is not required for the cell cycle arrest induced by absence of a sister chromatid. This finding is in contrast to a requirement for *MAD1* and *MAD2*.

### Discussion

The current biochemical model of spindle checkpoint function predicts an equal requirement for *MAD1*, *MAD2*, and *MAD3* in checkpoint-dependent cell cycle arrest. In yeast cells, anaphase progression is blocked by the inhibitory complex Mad2–Mad3–Bub3–Cdc20, the formation of which requires Mad1 (41). This model does not provide an explanation for functional differentiation among Mad proteins seen occasionally in chromosome loss assays, genetic interactions, and subcellular localizations (9, 10, 13, 15, 16). However, a functional difference is robustly supported by our genetic interaction analysis, which demonstrates a requirement for *MAD3* in only a subset of mutants that require *MAD1* and *MAD2*. This study shows that functional differentiation is not apparent under conditions where microtubules are globally destabilized by drug treatment, but is apparent when spindle structure is compromised by other stresses, provided by loss of the genes identified as synthetic lethal partners. Here, we show that budding yeast Mad1 and Mad2 are essential members of the cellular response to lack of bipolar orientation or tension, whereas Mad1, Mad2, and Mad3 are essential members of the response to global microtubule disruption. This observation in turn predicts that the null

mutants that equally require all three Mad proteins cause a spectrum of defects similar to nocodazole treatment, whereas mutants requiring *MAD3* less than *MAD1* or *MAD2* likely represent a class of mutants generating primary defects with strong effects on bipolar orientation and tension across kinetochores. Elsewhere we have shown that *mad1Δ* and *mad2Δ* mutants exhibit a higher frequency of chromosome missegregation than *mad3Δ* mutants (13). This finding suggests that the type of microtubule damage experienced by unperturbed yeast cells is most often a bipolar orientation or tension failure.

The G<sub>2</sub>/M cell cycle arrest induced by removing *CDC6* from cells (40) occurs in the presence of a bipolar spindle and requires the essential protein kinase Ipl1 (42). Ipl1 destabilizes syntelic kinetochore–microtubule interactions (where sister kinetochores are both bound by microtubules emanating from a single pole) by phosphorylating members of the Dam1 protein complex on one sister kinetochore (43). The Dam1 complex is a key mediator in the kinetochore–microtubule interaction (44–46). The Ipl1-induced release of one kinetochore–microtubule interaction results in monotelic attachment (where one sister kinetochore is attached to a microtubule emanating from a spindle pole, and the other sister has no microtubule attachment) and thus creates opportunities for appropriate bipolar attachment of sister kinetochores (47). Previous studies had indicated a requirement for *MAD2* and *MAD1* in this arrest (26, 40) but had not addressed the role of *MAD3*. We observe that *MAD1* and *MAD2*, but not *MAD3*, are required for signaling an arrest in the presence of monotelic kinetochores (Fig. 3).

Recently, budding yeast Mad2p, but not Mad3p, was shown to participate in the efficient establishment of tension in meiosis I after microtubule depolymerization (48). The defect we observe in *mad2* cells lacking tension may indicate that *mad2* meiotic cells lack a checkpoint signaling component in meiosis that promotes bipolar attachment, a signaling component that *mad3* mutants have. Based on these observations, we predict that the major defect in mutants that require only *MAD1* and *MAD2* is primarily bipolar orientation or tension (*chl4*, *ctf3*, *iml3*, *mcm16*, and *mcm22*). In support of this interpretation, a recent study indicates that cells containing a conditional allele of *OKP1* (an essential member of the kinetochore complex containing Ctf19, Mcm21, Ame1, Chl4, Iml3, Mcm16, Mcm22, and Ctf3; Fig. 1A) have defects in establishing tension across sister kinetochores (34).

Additional evidence exists for a function for Mad1 and Mad2, not shared with Mad3, in aiding in the repair of biorientation/tension defects. Alleles of *DAM1* (*dam1-1* and *dam1-11*) have been shown to arrest at nonpermissive temperature at the G<sub>2</sub>/M transition with undivided nuclei. In mutants at nonpermissive temperature, rapid movement of a GFP-marked centromere along the mitotic spindle axis indicates that kinetochores are competent to bind microtubules. However, the close association of the GFP-marked centromere with a single spindle pole, as well as the absence of separation of the marked sister centromeres, suggests monotelic kinetochore attachment (49). Both Mad2 and Bub1 are recruited to kinetochores in *dam1-1* mutants (9), providing additional evidence for some kinetochores being unattached. These two alleles of *DAM1*, which have defects in kinetochore biorientation/tension, have a more severe genetic interaction with *mad2* than with *mad3* (45).

Intriguingly, our observation that Mad3 is not required in budding yeast to arrest the cell cycle in response to sister kinetochore bipolar orientation and tension defects differs from results in metazoan systems, where kinetochore localization of BubR1/Mad3 is responsive to the tension state of sister kinetochores. The discrepancy may reveal a true evolutionary divergence in checkpoint operation. Vertebrate BubR1 differs from yeast Mad3 in that it has a kinase domain, indicating the presence of an additional protein function. Moreover, vertebrate kineto-

chores interact with multiple microtubules assembled in bundles whose structure may require additional regulation.

More work needs to be done to address the question of the function of yeast Mad3 during nocodazole-induced spindle checkpoint arrest. Our detailed analyses confirm that Mad1, Mad2, and Mad3 are equally required for cell cycle arrest in response to nocodazole even when kinetic parameters are measured. One possibility is that a nocodazole-induced checkpoint signal differs from a signal caused by a tension defect, because nocodazole may induce several types of damage, of which at least one requires Mad3 for cell cycle arrest. A suggestion of what that damage might be comes from a recent report that demonstrates a requirement for Mad3, but not Mad1 nor Mad2, in arresting fission yeast cells at metaphase due to a misaligned bipolar mitotic spindle (50). In this view, Mad3 is required to maintain APC inhibition when the spindle is misaligned, whereas Mad1/Mad2 is important for cell cycle arrest caused by biorientation/tension defects. Support for this idea can be found in previous biochemical characterization of checkpoint protein complexes.

Human BubR1 and Mad2 can form separate inhibitory complexes with Cdc20 *in vivo*, and these may provide complementary activities necessary for checkpoint arrest in the presence of microtubule damage (51). Furthermore, Fang (52) shows that the vertebrate quaternary complex (Mad2–BubR1/Mad3–Bub3–Cdc20) is a more potent inhibitor of the APC than Mad2–Cdc20 alone *in vitro*. Modulation of the spindle checkpoint response after different damages may include specialized activities of distinct complexes that coordinate signal strength and optimal repair.

We thank R. Irizarry for advice and discussions about microarray data analysis; J. Boeke, S. Ooi, X. Pan, D. Yuan, and S. Sookhai-Mahadeo for protocols and discussions; S. Biggins and K. Kitagawa for *cdc6* strains; D. Warren, C. Warren, O. Chen, and other members of the Spencer laboratory for advice and discussions; and S. Biggins, S. Michaelis, A. Hoyt, C. Doherty, C. Warren, M. Eckley, and C. Tiffany for critical reading of the manuscript. This work was supported by the National Institute of General Medical Sciences (F.A.S.).

1. Musacchio, A. & Hardwick, K. G. (2002) *Nat. Rev. Mol. Cell. Biol.* **3**, 731–741.
2. Li, R. & Murray, A. W. (1991) *Cell* **66**, 519–531.
3. Hoyt, M. A., Stearns, T. & Botstein, D. (1990) *Mol. Cell. Biol.* **10**, 223–234.
4. Nasmyth, K. (2002) *Science* **297**, 559–565.
5. Bernard, P., Hardwick, K. & Javerzat, J. P. (1998) *J. Cell Biol.* **143**, 1775–1787.
6. Ikui, A. E., Furuya, K., Yanagida, M. & Matsumoto, T. (2002) *J. Cell Sci.* **115**, 1603–1610.
7. Millband, D. N. & Hardwick, K. G. (2002) *Mol. Cell. Biol.* **22**, 2728–2742.
8. Kerscher, O., Crotti, L. B. & Basrai, M. A. (2003) *Mol. Cell. Biol.* **23**, 6406–6418.
9. Gillett, E. S., Espelin, C. W. & Sorger, P. K. (2004) *J. Cell Biol.* **164**, 535–546.
10. Iouk, T., Kerscher, O., Scott, R. J., Basrai, M. A. & Wozniak, R. W. (2002) *J. Cell Biol.* **159**, 807–819.
11. Skoufias, D. A., Andreassen, P. R., Lacroix, F. B., Wilson, L. & Margolis, R. L. (2001) *Proc. Natl. Acad. Sci. USA* **98**, 4492–4497.
12. Shannon, K. B., Canman, J. C. & Salmon, E. D. (2002) *Mol. Biol. Cell* **13**, 3706–3719.
13. Warren, C. D., Brady, D. M., Johnston, R. C., Hanna, J. S., Hardwick, K. G. & Spencer, F. A. (2002) *Mol. Biol. Cell* **13**, 3029–3041.
14. Hardwick, K. G., Johnston, R. C., Smith, D. L. & Murray, A. W. (2000) *J. Cell Biol.* **148**, 871–882.
15. Hardwick, K. G., Li, R., Mistrot, C., Chen, R. H., Dann, P., Rudner, A. & Murray, A. W. (1999) *Genetics* **152**, 509–518.
16. Cheeseman, I. M., Brew, C., Wolyniak, M., Desai, A., Anderson, S., Muster, N., Yates, J. R., Huffaker, T. C., Drubin, D. G. & Barnes, G. (2001) *J. Cell Biol.* **155**, 1137–1145.
17. Tong, A. H., Lesage, G., Bader, G. D., Ding, H., Xu, H., Xin, X., Young, J., Berriz, G. F., Brost, R. L., Chang, M., *et al.* (2004) *Science* **303**, 808–813.
18. Giaever, G., Chu, A. M., Ni, L., Connelly, C., Riles, L., Veronneau, S., Dow, S., Lucau-Danila, A., Anderson, K., Andre, B., *et al.* (2002) *Nature* **418**, 387–391.
19. Ooi, S. L., Shoemaker, D. D. & Boeke, J. D. (2003) *Nat. Genet.* **35**, 277–286.
20. Rose, M., Winston, F. & Hieter, P. (1990) *Methods in Yeast Genetics: A Laboratory Course Manual* (Cold Spring Harbor Lab. Press, Plainview, NY).
21. Tong, A. H. Y., Evangelista, M., Parsons, A. B., Xu, H., Bader, G. D., Page, N., Robinson, M., Raghibizadeh, S., Hogue, C. W. V., Bussey, H., *et al.* (2001) *Science* **294**, 2364–2368.
22. Ooi, S. L., Shoemaker, D. D. & Boeke, J. D. (2001) *Science* **294**, 2552–2556.
23. Bolstad, B. M., Irizarry, R. A., Astrand, M. & Speed, T. P. (2003) *Bioinformatics* **19**, 185–193.
24. Hanna, J. S., Kroll, E. S., Lundblad, V. & Spencer, F. A. (2001) *Mol. Cell. Biol.* **21**, 3144–3158.
25. Pangilinan, F. & Spencer, F. (1996) *Mol. Biol. Cell* **7**, 1195–1208.
26. Stern, B. M. & Murray, A. W. (2001) *Curr. Biol.* **11**, 1462–1467.
27. Saunders, W., Hornack, D., Lengyel, V. & Deng, C. (1997) *J. Cell Biol.* **137**, 417–431.
28. Tirnauer, J. S., O'Toole, E., Berrueta, L., Bierer, B. E. & Pellman, D. (1999) *J. Cell Biol.* **145**, 993–1007.
29. Hyland, K. M. (1998) *Biology* (Johns Hopkins Univ. Press, Baltimore).
30. Fleming, J. A., Vega, L. R. & Solomon, F. (2000) *Genetics* **156**, 69–80.
31. Geissler, S., Siegers, K. & Schiebel, E. (1998) *EMBO J.* **17**, 952–966.
32. Lee, L., Tirnauer, J. S., Li, J., Schuyler, S. C., Liu, J. Y. & Pellman, D. (2000) *Science* **287**, 2260–2262.
33. Measday, V., Hailey, D. W., Pot, I., Givan, S. A., Hyland, K. M., Cagney, G., Fields, S., Davis, T. N. & Hieter, P. (2002) *Genes Dev.* **16**, 101–113.
34. De Wulf, P., McAinsh, A. D. & Sorger, P. K. (2003) *Genes Dev.* **17**, 2902–2921.
35. Zeng, X., Kahana, J. A., Silver, P. A., Morphew, M. K., McIntosh, J. R., Fitch, I. T., Carbon, J. & Saunders, W. S. (1999) *J. Cell Biol.* **146**, 415–425.
36. Chen, R. H., Brady, D. M., Smith, D., Murray, A. W. & Hardwick, K. G. (1999) *Mol. Biol. Cell* **10**, 2607–2618.
37. Iwanaga, Y., Kasai, T., Kibler, K. & Jeang, K. T. (2002) *J. Biol. Chem.* **277**, 31005–31013.
38. Alexandru, G., Zachariae, W., Schleiffer, A. & Nasmyth, K. (1999) *EMBO J.* **18**, 2707–2721.
39. Straight, A. F., Belmont, A. S., Robinett, C. C. & Murray, A. W. (1996) *Curr. Biol.* **6**, 1599–1608.
40. Biggins, S. & Murray, A. W. (2001) *Genes Dev.* **15**, 3118–3129.
41. Brady, D. M. & Hardwick, K. G. (2000) *Curr. Biol.* **10**, 675–678.
42. Biggins, S., Severin, F. F., Bhalla, N., Sassoon, I., Hyman, A. A. & Murray, A. W. (1999) *Genes Dev.* **13**, 532–544.
43. Shang, C., Hazbun, T. R., Cheeseman, I. M., Aranda, J., Fields, S., Drubin, D. G. & Barnes, G. (2003) *Mol. Biol. Cell* **14**, 3342–3355.
44. Hofmann, C., Cheeseman, I. M., Goode, B. L., McDonald, K. L., Barnes, G. & Drubin, D. G. (1998) *J. Cell Biol.* **143**, 1029–1040.
45. Cheeseman, I. M., Enquist-Newman, M., Muller-Reichert, T., Drubin, D. G. & Barnes, G. (2001) *J. Cell Biol.* **152**, 197–212.
46. Jones, M. H., He, X., Giddings, T. H. & Winey, M. (2001) *Proc. Natl. Acad. Sci. USA* **98**, 13675–13680.
47. Tanaka, T. U., Rachidi, N., Janke, C., Pereira, G., Galova, M., Schiebel, E., Stark, M. J. & Nasmyth, K. (2002) *Cell* **108**, 317–329.
48. Shonn, M. A., Murray, A. L. & Murray, A. W. (2003) *Curr. Biol.* **13**, 1979–1984.
49. He, X., Rines, D. R., Espelin, C. W. & Sorger, P. K. (2001) *Cell* **106**, 195–206.
50. Tournier, S., Gachet, Y., Buck, V., Hyams, J. S. & Millar, J. B. (May 14, 2004) *Mol. Biol. Cell.*, mbc 10.1091 E04-03-0256.
51. Sudakin, V., Chan, G. K. & Yen, T. J. (2001) *J. Cell Biol.* **154**, 925–936.
52. Fang, G. (2002) *Mol. Biol. Cell* **13**, 755–766.